



Consensus of multi-agent systems with dynamic join characteristics under impulsive control*

Xiang HU¹, Zufan ZHANG¹, Chuandong LI^{‡2}

¹*School of Communication and Information Engineering,*

Chongqing University of Posts and Telecommunications, Chongqing 400065, China

²*Chongqing Key Laboratory of Nonlinear Circuits and Intelligent Information Processing,*

College of Electronic and Information Engineering, Southwest University, Chongqing 400715, China

E-mail: huyangyu0203@163.com; zhangzf@cqupt.edu.cn; cdli@swu.edu.cn

Received Feb. 6, 2020; Revision accepted Apr. 23, 2020; Crosschecked Sept. 28, 2020

Abstract: We study how to achieve the state consensus of a whole multi-agent system after adding some new agent groups dynamically in the original multi-agent system. We analyze the feasibility of dynamically adding agent groups under different forms of network topologies that are currently common, and obtain four feasible schemes in theory, including one scheme that is the best in actual industrial production. Then, we carry out dynamic modeling of multi-agent systems for the best scheme. Impulsive control theory and Lyapunov stability theory are used to analyze the conditions so that the whole multi-agent system with dynamic join characteristics can achieve state consensus. Finally, we provide a numerical example to verify the practicality and validity of the theory.

Key words: Multi-agent system; Network topology; Impulsive input; Dynamic join characteristics; State consensus

<https://doi.org/10.1631/FITEE.2000062>

CLC number: TP273

1 Introduction

In the past 20 years, multi-agent systems have attracted increasing attention. Usually, a multi-agent system consists of several agents, each of which has its own dynamic model. These agents are connected to each other through a network, and can communicate with their neighbors. After communication and control between the agents, the whole multi-agent system can work together efficiently. We call this collaborative working. As a special case of collaborative working of multi-agent systems,

state consensus of multi-agent systems has attracted greater interest. State consensus means that each agent needs to converge to the same state through a shared communication network. Studying state consensus, many scholars have proposed several dynamic models of multi-agent systems. Linear and nonlinear models are popular dynamic models. The linear models are simpler, and the nonlinear models are more complex but are closer to the actual industrial applications. Zhang Y and Tian (2014), Wang ZM et al. (2016), and Shi et al. (2019) studied mainly the state consensus of multi-agent systems based on linear models. Huang J et al. (2017), Han and Li (2018), Yuan et al. (2018), Wu et al. (2019), Ye and Su (2019), Zhang WB et al. (2019), and Huang C et al. (2020) studied mainly multi-agent systems based on nonlinear models. Since all agents need to communicate with each other, it is necessary to establish communication networks between them.

[‡] Corresponding author

* Project supported by the National Natural Science Foundation of China (No. 61873213), the Chongqing Graduate Research and Innovation Project in 2019, China (No. CYB19175), and the Major Project of Science and Technology Research Program of Chongqing Education Commission of China (No. KJZD-M201900601)

ORCID: Xiang HU, <https://orcid.org/0000-0002-1625-3825>; Chuandong LI, <https://orcid.org/0000-0001-6155-4849>

© Zhejiang University Press 2021

In the current study of communication networks of multi-agent systems, the research commonly involves fixed topology networks, switched topology networks, directed networks, and undirected networks. Fixed topology networks mean that communication connections between agents are always unchanged during the evolution of multi-agent systems. This method is simple and practical. Shang (2012), Xie and Wang (2012), and Lee and Bhattacharya (2016) studied mainly the state consensus of multi-agent systems with fixed topology networks. Switched topology networks mean that there are several modes of communication connections in the evolution process, and that communication connections of multi-agent systems will change from one mode to another according to some certain control rules. Jiang et al. (2010), Zhai and Yang (2014), Li CJ and Liu (2018a, 2018b), Lu et al. (2019), and Wen GH and Zheng (2019) studied mainly the state consensus with switched topology networks. Directed networks involve the direction of information transmission in the process of communication between agents. Wang H et al. (2018, 2019), Cheng et al. (2019), and Xu et al. (2019) studied mainly the state consensus based on directed networks. Undirected networks mean that information exchange between agents is directionless; that is, the information on each communication connection can be transmitted bidirectionally. Wang S and Xie (2012), Luo and Cao (2015), and Cao and Sun (2016) studied mainly the state consensus based on undirected networks.

Currently, scholars usually consider two implementation methods of average consensus and leader-following consensus. Average consensus means that after effective control, states of all agents will converge to the average value, and over time, the states of all agents will remain in consensus. The method of leader-following consensus usually selects an agent as the leader, and after effective control, the states of all agents will remain in consensus with the state of the leader. Hao and Chen (2012), Wang XM et al. (2018), Wang AJ et al. (2019), and Zheng et al. (2019) studied mainly the average consensus. Zhou and Liao (2014), Zou et al. (2019), Li YL et al. (2019), Wen GG et al. (2019), and Zhu et al. (2019) studied mainly the leader-following consensus.

As a key part of multi-agent systems, the communication control protocol can be realized by various algorithms. In these algorithms, impulsive con-

trol is effective. Impulsive control theory is usually used in the stability control of nonlinear and linear systems. At present, many scholars are studying the impulsive control theory. Huang TW et al. (2012), Wang X et al. (2014), Li YM et al. (2015), Sesekin and Nepp (2015), Li XD et al. (2017), Hu and Zhu (2018), and Liu et al. (2019) studied the control of nonlinear systems by some impulsive inputs. Geng and Duan (2007), Schoukens et al. (2018), Shahrrava (2018), Wang JR et al. (2018), and Wang YQ et al. (2019) studied the effect of impulsive control on linear systems. From the above studies, we can see that the time of impulse occurrence can be fixed or variable, and that even the existence of an impulse time window is considered. The intensity of impulses can be infinite in theory or be saturated. Therefore, impulsive control is a flexible control method, and has become a research hotspot.

Definition 1 (Dynamic join characteristics) The multi-agent systems with dynamic join characteristics mean that some agent groups work first, and then as time goes on, some new agent groups can randomly join. The new agent groups can communicate with the existing agent groups, but cannot affect the evolution states of the existing agent groups or the time for the existing agent groups to achieve state consensus.

We will make several combinations of the average consensus, leader-following consensus, directed networks, undirected networks, and impulsive control. We will analyze the feasibility of these combinations in multi-agent systems with dynamic join characteristics. We will discuss whether the four cases of average consensus with undirected networks, leader-following consensus with undirected networks, average consensus with directed networks, and leader-following consensus with directed networks support the dynamic join characteristics of multi-agent systems. We analyze the above four cases in detail and obtain four feasible schemes including the best one. We will establish the topology model of the communication network and the dynamic model of multi-agent systems based on the best scheme. Then, the dynamic model is analyzed by Lyapunov stability theory. The sufficient and necessary conditions of state consensus are obtained.

The main contributions of this paper are as follows:

1. To the best of our knowledge, we have

given the definition of dynamic join characteristics of multi-agent systems for the first time. It broadens the thinking and research scope of achieving state consensus in multi-agent systems.

2. Through analysis, we find a best scheme to support the state consensus of multi-agent systems with dynamic join characteristics from some common network topologies. This best scheme not only has theoretical value, but also integrates the concept of actual industrial production, and has high engineering significance.

3. Based on the best scheme, we establish a dynamic model of multi-agent systems and obtain some sufficient conditions of state consensus.

4. We give a numerical example through Matlab program to verify the practicality and validity of theoretical results.

2 Preliminaries

In this section, we will provide some notations, algebraic graph theories, and common dynamics models of multi-agent systems.

Notations: We use \mathbb{R} , \mathbb{R}^+ , $\mathbb{R}^{n \times n}$, and \mathbb{N}^+ to represent the set of real numbers, the set of positive real numbers, the set of $n \times n$ real matrices, and the set of positive integers, respectively. We denote $n \in \mathbb{N}^+$. $\lambda_M(\Omega)$ represents the maximum eigenvalue of matrix Ω , and $\lambda_m(\Omega)$ represents the smallest eigenvalue of matrix Ω . $\text{diag}(a_1, a_2, \dots, a_n)$ stands for an n -dimensional diagonal matrix. $|\cdot|$ and $\|\cdot\|$ represent the absolute value and Euclidean norm, respectively. I_n represents the n -dimensional identity matrix. x_k , x_{ki} , and $x_{ki}(t)$ represent the k^{th} agent group, the i^{th} agent in the k^{th} agent group, and the state of the i^{th} agent in the k^{th} agent group at time t , respectively, where $k, i \in \mathbb{N}^+$ and $t = 0$ or $t \in \mathbb{R}^+$.

Algebraic graph theories: Throughout this paper, communication networks are based on algebraic graph theories. Let $G=(\nu, \varepsilon)$ denote a connected graph with the set of nodes $\nu = \{1, 2, \dots, n\}$ and the set of edges $\varepsilon \subseteq \nu \times \nu$. $\mathbf{A} = [a_{ij}] \in \mathbb{R}^{n \times n}$ denotes the weighted adjacency matrix of the graph G with nonnegative elements, where $a_{ii} = 0$ and $a_{ij} \geq 0$ ($i \neq j$).

If G is an undirected graph without multiple edges and self-loops, we specify that all the elements of matrix \mathbf{A} contain only 0 or 1. If nodes i and j are connected, $a_{ij} = 1$; otherwise, $a_{ij} = 0$. The degree of

node i is defined by $\text{deg}(i) = \sum_{j=1}^n a_{ij}$ ($i = 1, 2, \dots, n$).

Let matrix $\mathbf{D} = \text{diag}(\text{deg}(1), \text{deg}(2), \dots, \text{deg}(n))$ be a diagonal matrix, and define it as the degree matrix of graph G . Then, the Laplacian matrix \mathbf{L} is defined as $\mathbf{L} = \mathbf{D} - \mathbf{A}$.

If G is a directed graph without multiple edges and self-loops, an edge rooted at node i and ended at node j is denoted by (i, j) . Denote $a_{ij} = 1$ if $(i, j) \in \varepsilon$; otherwise, $a_{ij} = 0$. We say that node j is a neighbor of node i if $(i, j) \in \varepsilon$. The out-degree of node i is defined as $\text{deg}(i) = \sum_{j=1}^n a_{ij}$ ($i = 1, 2, \dots, n$).

Let $\mathbf{D} = \text{diag}(\text{deg}(1), \text{deg}(2), \dots, \text{deg}(n))$ represent the degree matrix of the directed graph G . The Laplacian matrix \mathbf{L} is defined as $\mathbf{L} = \mathbf{D} - \mathbf{A}$. In a directed graph, a sequence of successive edges in the form of $(i, l), (l, m), \dots, (k, j)$ is a directed path from node i to node j . If there is a node (We call it a root node) in a directed graph that can reach all the other nodes in the graph through some directed paths, then we say that the directed graph has a spanning tree.

When we involve several agent groups, each agent group has its own communication network. Suppose that the communication network topology of the k^{th} agent group is G_k . Then we use $\mathbf{A}_k = [a_{kij}]$ to represent its weighted adjacency matrix. \mathbf{D}_k and $\mathbf{L}_k = \mathbf{D}_k - \mathbf{A}_k$ represent the degree matrix of G_k and the Laplacian matrix of G_k , respectively.

Common dynamics models of multi-agent systems: Generally, the establishment of dynamics models of multi-agent systems is usually restricted by multiple factors. Different means of controlling inputs and different schemes of achieving state consensus will result in a difference of dynamics models. In the schemes of multi-agent systems to achieve state consensus, this study involves average consensus and leader-following consensus. In the control inputs of multi-agent systems, impulsive theory is introduced. The common dynamics model of multi-agent systems can be described as

$$\dot{x}_{ki}(t) = \varpi(t, x_{ki}(t)) + u_{ki}(t), \quad (1)$$

where $x_{ki}(t)$ is the state value of agent i in the k^{th} agent group at time t and $\varpi(t, x_{ki}(t))$ is a function with t and $x_{ki}(t)$ as variables. $u_{ki}(t)$ is the control input of agent i in the k^{th} agent group at time t , and

can be defined as

$$u_{ki}(t) = \sum_{m=1}^{\infty} f_k \left(\sum_{kj \in \Xi_{ki}} a_{kij} [x_{ki}(t) - x_{kj}(t)] + b_{ki} [x_{ki}(t) - x_0(t)] \right) \delta(t - t_{km}), \quad (2)$$

where f_k is the impulse strength to the k^{th} agent group, Ξ_{ki} represents the set of neighbor nodes of agent i in the k^{th} agent group, and $x_0(t)$ is the state value of a leader agent. Let b_{ki} be the weight of the edge from the leader agent to the i^{th} agent in the k^{th} agent group, and $b_{ki} > 0$ if and only if there is an edge from the leader agent to agent i in the k^{th} agent group. As is normally considered to be the case, when there is an edge from the leader agent to agent i in the k^{th} agent group, $b_{ki} = 1$ will be directly defined in this study. $b_{ki} = 0$ means that there is no connection edge between the leader agent and agent i in the k^{th} agent group. Clearly, if all the agents in the k^{th} agent group have no leader agent, then $b_{ki} = 0$ ($i = 1, 2, \dots$). We denote $\delta(\cdot)$ a Dirac function. The non-negative real number t_{km} represents the time when the impulse occurs, and its detailed definition can vary with the impulsive control strategy, which we will define in detail later in this paper. We can also call $u_{ki}(t)$ a control protocol.

Assumption 1 Continuous nonlinear function $\varphi : R \rightarrow R$ satisfies the Lipschitz condition:

$$|\varphi(x_1) - \varphi(x_2)| \leq l|x_1 - x_2|, \quad (3)$$

where l is the Lipschitz constant.

3 Feasibility of several schemes

Some currently common network topologies are not suitable for the implementation of state consensus of multi-agent systems with dynamic join characteristics. In this section, we will analyze the network topologies and find out several implementation schemes suitable for the dynamic join characteristics.

This section involves the combination analysis of directed networks, undirected networks, average consensus, and leader-following consensus.

3.1 Average consensus with undirected networks

In this subsection, we will consider whether the combination of average consensus and undirected

networks can support the implementation of state consensus of multi-agent systems with dynamic join characteristics. Fig. 1 shows a dynamic joining topology of multi-agent systems based on average consensus with undirected networks.

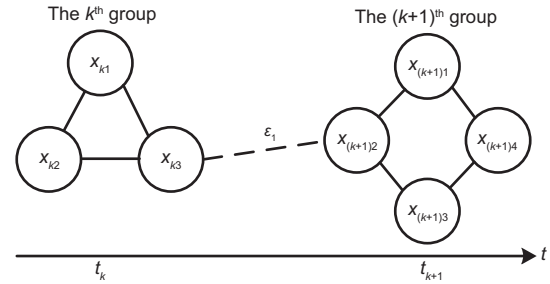


Fig. 1 Dynamic joining topology of multi-agent systems based on average consensus with undirected networks

At time t_k , we assume that the k^{th} agent group has started working. At time t_{k+1} , we dynamically join the $(k + 1)^{\text{th}}$ agent group, and communications between all the agents are based on an undirected network. From Fig. 1, we can see that there is an undirected edge ε_1 between agent x_{k3} in the k^{th} agent group and agent $x_{(k+1)2}$ in the $(k + 1)^{\text{th}}$ agent group.

Case 1: At time t_{k+1} , agents in the k^{th} agent group have not achieved state consensus. Since agent x_{k3} in the k^{th} agent group and agent $x_{(k+1)2}$ in the $(k + 1)^{\text{th}}$ agent group are connected by ε_1 , it can be seen from Eqs. (1) and (2) and Fig. 1 that the k^{th} and $(k + 1)^{\text{th}}$ agent groups will affect each other due to the existence of $\sum_{m=1}^{\infty} f_k \left(\sum_{kj \in \Xi_{ki}} a_{kij} [x_{ki}(t) - x_{kj}(t)] \right)$, $\sum_{m=1}^{\infty} f_k (x_{k3}(t) - x_{(k+1)2}(t))$, $\sum_{m=1}^{\infty} f_{k+1} (x_{(k+1)2}(t) - x_{k3}(t))$, and $\sum_{m=1}^{\infty} f_{k+1} \left(\sum_{(k+1)j \in \Xi_{(k+1)i}} a_{(k+1)ij} [x_{(k+1)i}(t) - x_{(k+1)j}(t)] \right)$. This may delay the time when the k^{th} agent group achieves state consensus. In extreme cases, more and more other agent groups are continuously added, and the newly added agent groups will be connected with the existing ones through several undirected edges. Then, the newly added agent groups may always delay the time when the existing agent groups achieve state consensus. Therefore, this situation does not conform to the feasibility and efficiency principles of actual industrial production.

Case 2: At time t_{k+1} , agents in the k^{th} agent group have achieved state consensus. Since agent

x_{k3} in the k^{th} agent group and agent $x_{(k+1)2}$ in the $(k+1)^{\text{th}}$ agent group are connected by an undirected edge ε_1 , it can be seen from Eqs. (1) and (2) and Fig. 1 that the state of the $(k+1)^{\text{th}}$ agent group will affect that of the k^{th} agent group due to the existence of $\sum_{m=1}^{\infty} f_k \left(\sum_{kj \in \Xi_{ki}} a_{kij} [x_{ki}(t) - x_{kj}(t)] \right)$ and $\sum_{m=1}^{\infty} f_k (x_{k3}(t) - x_{(k+1)2}(t))$. This will lead to the states not having consensus again in the k^{th} agent group, which obviously does not conform to the needs of actual industrial production.

Therefore, the scheme of “average consensus with undirected networks” is not suitable for the state consensus study of multi-agent systems with dynamic join characteristics.

3.2 Average consensus with directed networks

In this subsection, we will consider whether the combination of average consensus and directed networks can support the implementation. Fig. 2 shows a dynamic joining topology of multi-agent systems based on average consensus with directed networks.

At time t_k , we assume that the k^{th} agent group has started working. At time t_{k+1} , we dynamically join the $(k+1)^{\text{th}}$ agent group, and communication between these agents is based on a directed network. From Fig. 2, we can see that there is a directed edge ε_1 (or ε_2 or ε_3) between agent x_{k3} in the k^{th} agent group and agent $x_{(k+1)2}$ in the $(k+1)^{\text{th}}$ agent group.

Case 1: The directed edge connecting agent x_{k3} in the k^{th} agent group to agent $x_{(k+1)2}$ in the $(k+1)^{\text{th}}$ agent group is ε_1 , and ε_1 is bidirectional. Since the k^{th} and $(k+1)^{\text{th}}$ agent groups can affect each other, this scheme is similar to the scheme of “average consensus with undirected network” and is not feasible.

Case 2: The directed edge connecting agent x_{k3}

in the k^{th} agent group to agent $x_{(k+1)2}$ in the $(k+1)^{\text{th}}$ agent group is ε_2 , and ε_2 is one-way. The information can be sent only from agent $x_{(k+1)2}$ in the $(k+1)^{\text{th}}$ agent group to agent x_{k3} in the k^{th} agent group. In this situation, the $(k+1)^{\text{th}}$ agent group will affect the k^{th} agent group. This scheme is also similar to the scheme of “average consensus with undirected network” and is not feasible.

Case 3: The directed edge connecting agent x_{k3} in the k^{th} agent group to agent $x_{(k+1)2}$ in the $(k+1)^{\text{th}}$ agent group is ε_3 , and ε_3 is one-way. The information can be sent only from agent x_{k3} in the k^{th} agent group to agent $x_{(k+1)2}$ in the $(k+1)^{\text{th}}$ agent group. In this situation, the k^{th} agent group will affect the $(k+1)^{\text{th}}$ agent group, and the $(k+1)^{\text{th}}$ agent group will not affect the k^{th} agent group. Similarly, the $(k+2)^{\text{th}}$ agent group, $(k+3)^{\text{th}}$ agent group, $(k+4)^{\text{th}}$ agent group, and so on, can be added dynamically in sequence. As long as the newly added agent groups are connected to the existing agent groups in the manner of the directed edge ε_3 , through effective control, all agent groups will be able to achieve state consensus, and the newly added agent groups will not delay the time when the existing agent groups achieve state consensus. However, in the actual industrial application, there are still some problems in this situation. For example, if the k^{th} and $(k+1)^{\text{th}}$ agent groups already exist, then we dynamically add the $(k+2)^{\text{th}}$ agent group. We could connect just the newly added $(k+2)^{\text{th}}$ agent group to the existing k^{th} agent group in the manner of the directed edge ε_3 , or we could connect just the newly added $(k+2)^{\text{th}}$ agent group to the existing $(k+1)^{\text{th}}$ agent group in the manner of the directed edge ε_3 , or we could connect the newly added $(k+2)^{\text{th}}$ agent group to both the k^{th} and $(k+1)^{\text{th}}$ agent groups in the manner of the directed edge ε_3 . Then, we need to formulate a rule to specify the specific connection mode between the newly added agent groups and the existing ones. This is cumbersome. Another obvious disadvantage of this situation is that the newly added agent groups will have communication edges with the existing agent groups. As a large number of newly added agent groups are added, there will be a communication burden on the existing agent groups, and this will be a serious problem in the actual industrial situation. Based on the above analysis, we know that this situation is feasible in theory, but it is not suitable for actual industrial production.

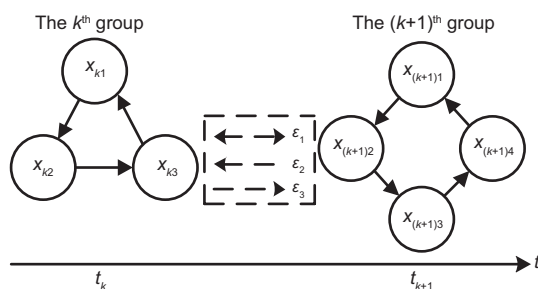


Fig. 2 Dynamic joining topology of multi-agent systems based on average consensus with directed networks

3.3 Leader-following consensus with undirected networks

In this subsection, we will consider whether the combination of leader-following consensus with undirected networks can support the implementation we are seeking for.

Case 1: Fig. 3 shows a dynamic joining topology of multi-agent systems based on leader-following consensus with undirected networks.

At time t_0 , we assume that the leader agent has started working. At time t_k , we dynamically join the k^{th} agent group. At time t_{k+1} , we dynamically join the $(k + 1)^{\text{th}}$ agent group. From Fig. 3, we can see that the leader agent is connected to the k^{th} and $(k + 1)^{\text{th}}$ agent groups by directed edges ε_1 and ε_2 , respectively. The direction of information transformation on ε_1 is from the leader agent to the k^{th} agent group, and the direction of information transformation on ε_2 is from the leader agent to the $(k + 1)^{\text{th}}$ agent group. All the other agents are connected to each other by the undirected edges. Agent x_{k1} in the k^{th} agent group and agent $x_{(k+1)2}$ in the $(k + 1)^{\text{th}}$ agent group are connected by the undirected edge ε_3 . In this way, the $(k + 1)^{\text{th}}$ agent group will affect the k^{th} agent group, which is similar to the scheme of “average consensus with undirected network” mentioned above, and is suitable for actual industrial production.

Case 2: Fig. 4 shows another dynamic joining topology based on leader-following consensus with undirected networks.

At time t_0 , we assume that the leader agent has started working. At time t_k , we dynamically join the k^{th} agent group. At time t_{k+1} , we dynamically join the $(k + 1)^{\text{th}}$ agent group. From Fig. 4, we can see that the leader agent is connected to the k^{th} and

$(k + 1)^{\text{th}}$ agent groups by directed edges ε_1 and ε_2 , respectively. The direction of information transformation on ε_1 is from the leader agent to the k^{th} agent group. The direction of information transformation on ε_2 is from the leader agent to the $(k + 1)^{\text{th}}$ agent group. All the other agents are connected to each other by undirected edges, and there is no connected communication edges between the k^{th} and $(k + 1)^{\text{th}}$ agent groups. In this way, the k^{th} and $(k + 1)^{\text{th}}$ agent groups will not affect each other, and they are affected only by the leader agent. After a period of effective communication control, they can achieve state consensus with the leader agent. If this scheme is adopted, the newly added agent groups will not delay the time for the existing agent groups to achieve state consensus or destroy the state consensus of the existing agent groups. We know that there are no communication connections between each agent group; that is, each agent group has communication connections only with the leader agent, and the other communication connections in each agent group are only internal connections. So, this situation avoids the communication burden between each agent group, and agents in different groups can also avoid collisions. Based on the above analysis, we basically do not need to strengthen the communication skills of the agents in each agent group. We need to strengthen only the communication skills of the leader agent, because the leader agent will communicate with all the agent groups. In this way, we avoid enhancing the communication skills of all agent groups, which will greatly reduce the communication burden and the production cost. Furthermore, the adoption of this scheme has the advantage of unified form for the state consensus problem of a single group and multiple groups. It meets the “KISS”

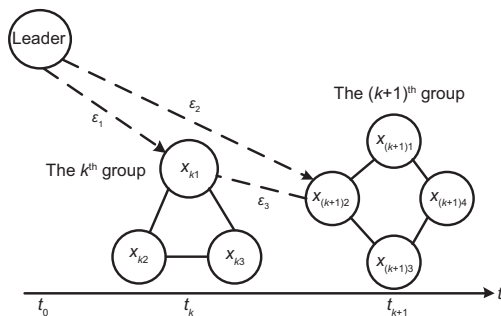


Fig. 3 Dynamic joining topology of multi-agent systems based on leader-following consensus with undirected networks

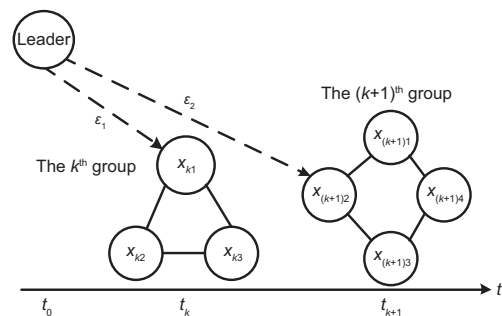


Fig. 4 Another dynamic joining topology of multi-agent systems based on leader-following consensus with undirected networks

(Keep It Simple, Stupid) principle in actual industrial production. Therefore, we take this scheme as the best one.

3.4 Leader-following consensus with directed networks

In this subsection, we will consider whether the combination of leader-following consensus with directed networks can support the implementation of state consensus of multi-agent systems with dynamic join characteristics.

Case 1: Fig. 5 shows a dynamic joining topology of multi-agent systems based on leader-following consensus with directed networks.

At time t_0 , we assume that the leader agent has started working. At time t_k , we dynamically join the k^{th} agent group. At time t_{k+1} , we dynamically join the $(k+1)^{\text{th}}$ agent group. From Fig. 5, we can see that the leader agent is connected to the k^{th} and $(k+1)^{\text{th}}$ agent groups by directed edges ε_1 and ε_2 , respectively. The direction of information transformation on ε_1 is from the leader agent to the k^{th} agent group, and the direction of information transformation on ε_2 is from the leader agent to the $(k+1)^{\text{th}}$ agent group. The connected communication edges of the k^{th} and $(k+1)^{\text{th}}$ agent groups are all directed edges, and there are no connected communication edges between the k^{th} and $(k+1)^{\text{th}}$ agent groups. We can see that this situation is similar to case 2 in Section 3.3, except that the internal communications of each agent group are directed edges. So, this situation is feasible in theory. Because the communication capability of the current communication equipment is relatively strong, the communication equipment generally supports one-to-many and two-way communications. So, in actual industrial

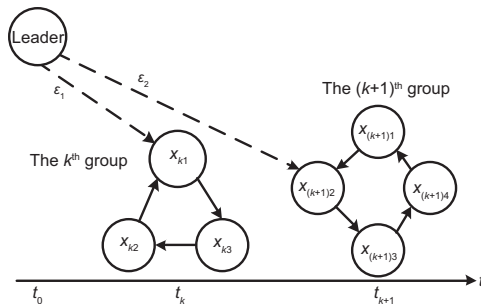


Fig. 5 Dynamic joining topology of multi-agent systems based on leader-following consensus with directed networks

production, if directed communication is adopted, the communication capability of the communication equipment cannot be maximized. Therefore, we do not consider this situation as a best one.

Case 2: Fig. 6 shows another dynamic joining topology based on leader-following consensus with directed networks.

As can be seen from Fig. 6, this situation is basically the same as that in Fig. 5, except that there is a directed edge $\varepsilon_3, \varepsilon_4$, or ε_5 between the k^{th} and $(k+1)^{\text{th}}$ agent groups in Fig. 6.

Through the previous analysis in this study, it is clear that if there is a directed edge ε_3 or ε_4 between the k^{th} and $(k+1)^{\text{th}}$ agent groups, since the state of the $(k+1)^{\text{th}}$ agent group will affect that of the k^{th} agent group, it does not meet the requirements of this study.

If the connected communication edge between the k^{th} and $(k+1)^{\text{th}}$ agent groups is the directed edge ε_5 , since the $(k+1)^{\text{th}}$ agent group will not affect the state of the k^{th} agent group, it meets the requirements in theory. In this situation, when the $(k+2)^{\text{th}}$ agent group, $(k+3)^{\text{th}}$ agent group, $(k+4)^{\text{th}}$ agent group, and so on, are added dynamically in sequence, there are many directed edges between all the agent groups. This is similar to case 3 in Section 3.2 and increases the communication burden of all agent groups. Similarly, since the communication between all agent groups of directed communication is adopted for the method, the communication capability of the communication equipment cannot be maximized. So, it is not a best scheme in actual industrial production.

In this section, we analyze mainly whether the currently common network topologies of multi-agent systems are suitable for the implementation we are

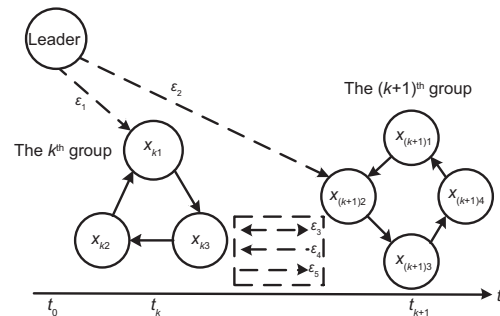


Fig. 6 Another dynamic joining topology of multi-agent systems based on leader-following consensus with directed networks

seeking for. Through the analysis in this section, we know that case 3 in Section 3.2, case 2 in Section 3.3, case 1 in Section 3.4, and case 2 with ε_5 in Section 3.4 are all feasible in theory. Among the four feasible schemes, case 2 in Section 3.3 can not only minimize the communication burden between agent groups, but also maximize the communication capability of each agent. So, in actual industrial production, the best scheme is case 2 in Section 3.3.

4 Problem formulation

Based on the scheme of case 2 in Section 3.3, let k and i be two positive integers. Assume that there are n ($n \in \mathbb{N}^+$) agent groups and that the k^{th} ($k \in [1, n]$) agent group has N_k ($N_k \in \mathbb{N}^+$) agents. We use $x_{ki}(t)$ to represent the state of the i^{th} ($i \in [1, N_k]$) agent in the k^{th} agent group at time t ($t = 0$ or $t \in \mathbb{R}^+$). We use x_0 to represent a leader agent, and all other agent groups can obtain information from the leader agent. We consider the communication network topology of each agent group as an undirected graph, and the dynamics of the leader agent and all other agents is nonlinear. The dynamics of the leader agent is described as follows:

$$\dot{x}_0(t) = Hx_0(t) + \varphi(x_0(t)), \tag{4}$$

where $H \in \mathbb{R}$, and $x_0(t) \in \mathbb{R}$ is the state of the leader agent. $\varphi(\cdot)$ is a continuous nonlinear function whose definition and properties have been given in Assumption 1. We assume that the leader agent x_0 starts working at t_0 .

Let $\varpi(t, x_{ki}(t)) = Hx_{ki}(t) + \varphi(x_{ki}(t))$. According to the common dynamics model (1), the dynamics of the i^{th} agent in the k^{th} agent group can be described as follows:

$$\dot{x}_{ki}(t) = Hx_{ki}(t) + \varphi(x_{ki}(t)) + u_{ki}(t), \tag{5}$$

where $k \in [1, n]$, $i \in [1, N_k]$, $x_{ki}(t) \in \mathbb{R}$ is the state of the i^{th} agent in the k^{th} agent group, and $u_{ki}(t)$ has been defined in Eq. (2). Although there are many common forms of impulse at present, such as event-based impulse, variable time impulse, and impulse with time windows, considering that this study is based mainly on dynamic join characteristics and the KISS principle in actual industrial production, we choose Eq. (2) as the control protocol. Of course, some more complex control methods can be considered in further research. Therefore, the dynamics (5)

can be rewritten as

$$\begin{aligned} \dot{x}_{ki}(t) = & Hx_{ki}(t) + \varphi(x_{ki}(t)) \\ & + \sum_{m=1}^{\infty} f_k \left(\sum_{kj \in \Xi_{ki}} a_{kij} [x_{ki}(t) - x_{kj}(t)] \right. \\ & \left. + b_{ki} [x_{ki}(t) - x_0(t)] \right) \delta(t - t_{km}). \end{aligned} \tag{6}$$

Assume that the k^{th} agent group is dynamically joined at time t_k , the $(k + 1)^{\text{th}}$ agent group is dynamically joined at time t_{k+1} , the $(k + 2)^{\text{th}}$ agent group is dynamically joined at time t_{k+2} , and so on. Clearly, $0 \leq t_0 \leq t_k \leq t_{k+1} \leq t_{k+2} \leq \dots \leq +\infty$. Assume that $\Delta x_{ki}(t_{km}) = x_{ki}(t_{km}^+) - x_{ki}(t_{km}^-)$, $x_{ki}(t_{km}) = x_{ki}(t_{km}^+)$, $x_{ki}(t_{km}^-) = \lim_{t \rightarrow t_{km}^-} x_{ki}(t)$, and $x_{ki}(t_{km}^+) = \lim_{t \rightarrow t_{km}^+} x_{ki}(t)$. Because the Dirac function $\delta(\cdot)$ has the property of $\int_{a-\Delta}^{a+\Delta} g(t)\delta(t - a)dt = g(a)$ for $\Delta \neq 0$, the dynamics (6) can be rewritten as

$$\begin{cases} \dot{x}_{ki}(t) = Hx_{ki}(t) + \varphi(x_{ki}(t)), & t \neq t_{km}, \\ \Delta x_{ki}(t_{km}) = f_k \left(\sum_{kj \in \Xi_{ki}} a_{kij} [x_{ki}(t_{km}^-) - x_{kj}(t_{km}^-)] \right. \\ \quad \left. + b_{ki} [x_{ki}(t_{km}^-) - x_0(t_{km}^-)] \right), & t = t_{km}, \end{cases} \tag{7}$$

where $k \in [1, n]$ and $i \in [1, N_k]$. We use a periodic control method to control each agent group, and let $T \in \mathbb{R}^+$ be the system control period. Let $t_{km} = t_k + mT + T/2$, where $m = 0$ or $m \in \mathbb{N}^+$.

Let the state error of the i^{th} agent in the k^{th} agent group be $e_{ki}(t) = x_{ki}(t) - x_0(t)$, and let the state error of the k^{th} agent group be $e_k(t) = [e_{k1}(t), e_{k2}(t), \dots, e_{kN_k}(t)]^T$. We can obtain

$$\begin{cases} \dot{e}_{ki}(t) = He_{ki}(t) + \varphi(x_{ki}(t)) - \varphi(x_0(t)), & t \neq t_{km}, \\ \Delta e_{ki}(t_{km}) = f_k \left(\sum_{kj \in \Xi_{ki}} a_{kij} [x_{ki}(t_{km}^-) - x_{kj}(t_{km}^-)] \right. \\ \quad \left. + b_{ki} [x_{ki}(t_{km}^-) - x_0(t_{km}^-)] \right), & t = t_{km}. \end{cases} \tag{8}$$

The error system is

$$\begin{cases} \dot{e}_k(t) = (I_{N_k} \otimes H)e_k(t) \\ \quad + \Psi_k(x_k(t), x_0(t)), & t \neq t_{km}, \\ e_k(t_{km}) = [I_{N_k} + f_k(L_k + B_k)]e_k(t_{km}^-), & t = t_{km}, \end{cases} \tag{9}$$

where $B_k = \text{diag}(b_{k1}, b_{k2}, \dots, b_{kN_k}) \in \mathbb{R}^{N_k \times N_k}$ and $\Psi_k(x_k(t), x_0(t)) = [\varphi(x_{k1}(t)) - \varphi(x_0(t)), \varphi(x_{k2}(t)) -$

$\varphi(x_0(t)), \dots, \varphi(x_{kN_k}(t)) - \varphi(x_0(t))\]^T$ ($k \in [1, n]$). The communication network topology of the k^{th} agent group is G_k , and L_k represents the Laplacian matrix of G_k .

Definition 2 For system (7), the system can achieve state consensus under control protocol (2) when

$$\lim_{t \rightarrow +\infty} |x_{ki}(t) - x_0(t)| = 0, \quad k \in [1, n], \quad i \in [1, N_k]. \tag{10}$$

5 Main results

In this section, theoretical analysis is provided for the state consensus problem of multi-agent systems with dynamic join characteristics under impulsive control.

Theorem 1 Suppose that there exists a positive constant $\eta_k > 0$ ($k \in [1, n]$). If the following inequalities hold:

- (1) $I_{N_k} \otimes (2H + 2I - \eta_k) \leq 0$,
- (2) $ln\lambda_k + \eta_k T < 0$,

where $\lambda_k = \lambda_M\{[I_{N_k} + f_k(L_k + B_k)]^T [I_{N_k} + f_k(L_k + B_k)]\}$, then the multi-agent system (7) can achieve state consensus under control protocol (2).

Proof First, we can construct the following Lyapunov function for error system (9):

$$V_k(e_k(t)) = e_k^T(t)e_k(t). \tag{11}$$

If $t \in (t_k + mT, t_k + mT + T/2)$, we have

$$\begin{aligned} \dot{V}_k(e_k(t)) &= 2e_k^T(t)\dot{e}_k(t) \\ &= 2e_k^T(t)[(I_{N_k} \otimes H)e_k(t) \\ &\quad + \Psi_k(x_k(t), x_0(t))] \\ &= 2e_k^T(t)(I_{N_k} \otimes H)e_k(t) \\ &\quad + 2e_k^T(t)\Psi_k(x_k(t), x_0(t)) \\ &\leq 2e_k^T(t)(I_{N_k} \otimes H)e_k(t) + 2e_k^T(t)le_k(t) \\ &\leq e_k^T(t)[I_{N_k} \otimes (2H + 2I)]e_k(t) \\ &\leq \eta_k V_k(e_k(t)) \\ &\quad + e_k^T(t)[I_{N_k} \otimes (2H + 2I - \eta_k)]e_k(t) \\ &\leq \eta_k V_k(e_k(t)). \end{aligned}$$

So,

$$V_k(e_k(t)) \leq V_k(e_k((t_k + mT)^+))\exp[\eta_k(t - t_k - mT)]. \tag{12}$$

If $t = t_{km}$, that is $t = t_k + mT + T/2$, we have

$$\begin{aligned} V_k(e_k(t_{km})) &= e_k^T(t_{km})e_k(t_{km}) \\ &= \{[I_{N_k} + f_k(L_k + B_k)]e_k(t_{km}^-)\}^T \\ &\quad \cdot \{[I_{N_k} + f_k(L_k + B_k)]e_k(t_{km}^-)\} \\ &= e_k^T(t_{km}^-)[I_{N_k} + f_k(L_k + B_k)]^T \\ &\quad \cdot [I_{N_k} + f_k(L_k + B_k)]e_k(t_{km}^-) \\ &\leq \lambda_k V_k(e_k(t_{km}^-)), \end{aligned} \tag{13}$$

where $\lambda_k = \lambda_M\{[I_{N_k} + f_k(L_k + B_k)]^T [I_{N_k} + f_k(L_k + B_k)]\}$.

If $t \in (t_{km}^+, t_k + (m + 1)T)$, similarly, we have

$$\dot{V}_k(e_k(t)) \leq \eta_k V_k(e_k(t)).$$

So,

$$\begin{aligned} V_k(e_k(t)) &\leq V_k(e_k(t_{km}^+))\exp[\eta_k(t - t_{km}^+)] \\ &\leq V_k(e_k((t_k + mT + T/2)^+)) \\ &\quad \cdot \exp[\eta_k(t - t_k - mT - T/2)]. \end{aligned} \tag{14}$$

We can do the following mathematical induction through inequalities (12)–(14):

Case 1: $m = 0$.

Subcase 1: If $t \in (t_k, t_k + T/2)$, then we can obtain

$$V_k(e_k(t)) \leq V_k(e_k(t_k^+))\exp[\eta_k(t - t_k)].$$

So, $V_k(e_k((t_k + T/2)^-)) \leq V_k(e_k(t_k^+))\exp[\eta_k(T/2)]$.

Subcase 2: If $t = t_{k0}$, that is $t = t_k + T/2$, then we can obtain

$$\begin{aligned} V_k(e_k(t))|_{t=t_k+T/2} &\leq \lambda_k V_k(e_k((t_k + T/2)^-)) \\ &\leq \lambda_k V_k(e_k(t_k^+))\exp[\eta_k(T/2)]. \end{aligned}$$

Subcase 3: If $t \in (t_k + T/2, t_k + T)$, then we can obtain

$$\begin{aligned} V_k(e_k(t)) &\leq V_k(e_k((t_k + T/2)^+))\exp[\eta_k(t - t_k - T/2)] \\ &\leq \lambda_k V_k(e_k(t_k^+))\exp(\eta_k(T/2)) \\ &\quad \cdot \exp[\eta_k(t - t_k - T/2)] \\ &\leq \lambda_k V_k(e_k(t_k^+))\exp[\eta_k(t - t_k)]. \end{aligned}$$

So, $V_k(e_k(t_k + T)) \leq \lambda_k V_k(e_k(t_k^+))\exp[\eta_k(T)]$.

Case 2: $m = 1$.

Subcase 1: If $t \in (t_k + T, t_k + 3T/2)$, then we can obtain

$$\begin{aligned} V_k(e_k(t)) &\leq V_k(e_k((t_k + T)^+))\exp[\eta_k(t - t_k - T)] \\ &\leq \lambda_k V_k(e_k(t_k^+))\exp[\eta_k(T)] \\ &\quad \cdot \exp[\eta_k(t - t_k - T)] \\ &\leq \lambda_k V_k(e_k(t_k^+))\exp[\eta_k(t - t_k)]. \end{aligned}$$

So, $V_k(\mathbf{e}_k((t_k + 3T/2)^-)) \leq \lambda_k V_k(\mathbf{e}_k(t_k^+)) \cdot \exp[\eta_k(3T/2)]$.

Subcase 2: If $t = t_{k1}$, that is $t = t_k + 3T/2$, then we can obtain

$$V_k(\mathbf{e}_k(t))|_{t=t_k+3T/2} \leq \lambda_k V_k(\mathbf{e}_k((t_k + 3T/2)^-)) \leq \lambda_k^2 V_k(\mathbf{e}_k(t_k^+)) \exp[\eta_k(3T/2)].$$

Subcase 3: If $t \in (t_k + 3T/2, t_k + 2T]$, then we can obtain

$$\begin{aligned} V_k(\mathbf{e}_k(t)) &\leq V_k(\mathbf{e}_k((t_k + 3T/2)^+)) \\ &\quad \cdot \exp[\eta_k(t - t_k - 3T/2)] \\ &\leq \lambda_k^2 V_k(\mathbf{e}_k(t_k^+)) \exp[\eta_k(3T/2)] \\ &\quad \cdot \exp[\eta_k(t - t_k - 3T/2)] \\ &\leq \lambda_k^2 V_k(\mathbf{e}_k(t_k^+)) \exp[\eta_k(t - t_k)]. \end{aligned}$$

So, $V_k(\mathbf{e}_k(t_k + 2T)) \leq \lambda_k^2 V_k(\mathbf{e}_k(t_k^+)) \exp[\eta_k(2T)]$.

Case 3: $m = 2$.

Subcase 1: If $t \in (t_k + 2T, t_k + 5T/2)$, then we can obtain

$$\begin{aligned} V_k(\mathbf{e}_k(t)) &\leq V_k(\mathbf{e}_k((t_k + 2T)^+)) \exp[\eta_k(t - t_k - 2T)] \\ &\leq \lambda_k^2 V_k(\mathbf{e}_k(t_k^+)) \exp[\eta_k(2T)] \\ &\quad \cdot \exp[\eta_k(t - t_k - 2T)] \\ &\leq \lambda_k^2 V_k(\mathbf{e}_k(t_k^+)) \exp[\eta_k(t - t_k)]. \end{aligned}$$

So, $V_k(\mathbf{e}_k((t_k + 5T/2)^-)) \leq \lambda_k^2 V_k(\mathbf{e}_k(t_k^+)) \cdot \exp[\eta_k(5T/2)]$.

Subcase 2: If $t = t_{k2}$, that is $t = t_k + 5T/2$, then we can obtain

$$V_k(\mathbf{e}_k(t))|_{t=t_k+5T/2} \leq \lambda_k V_k(\mathbf{e}_k((t_k + 5T/2)^-)) \leq \lambda_k^3 V_k(\mathbf{e}_k(t_k^+)) \exp[\eta_k(5T/2)].$$

Subcase 3: If $t \in (t_k + 5T/2, t_k + 3T]$, then we can obtain

$$\begin{aligned} V_k(\mathbf{e}_k(t)) &\leq V_k(\mathbf{e}_k((t_k + 5T/2)^+)) \\ &\quad \cdot \exp[\eta_k(t - t_k - 5T/2)] \\ &\leq \lambda_k^3 V_k(\mathbf{e}_k(t_k^+)) \exp[\eta_k(5T/2)] \\ &\quad \cdot \exp[\eta_k(t - t_k - 5T/2)] \\ &\leq \lambda_k^3 V_k(\mathbf{e}_k(t_k^+)) \exp[\eta_k(t - t_k)]. \end{aligned}$$

So, $V_k(\mathbf{e}_k(t_k + 3T)) \leq \lambda_k^3 V_k(\mathbf{e}_k(t_k^+)) \exp[\eta_k(3T)]$.

Case $\theta + 1$: $m = \theta$ ($\theta \in \mathbb{N}^+$).

Subcase 1: If $t \in (t_k + \theta T, t_k + \theta T + T/2)$, then we can obtain

$$V_k(\mathbf{e}_k(t)) \leq \lambda_k^\theta V_k(\mathbf{e}_k(t_k^+)) \exp[\eta_k(t - t_k)]. \quad (15)$$

Subcase 2: If $t \in [t_k + \theta T + T/2, t_k + (\theta + 1)T]$, then we can obtain

$$V_k(\mathbf{e}_k(t)) \leq \lambda_k^{\theta+1} V_k(\mathbf{e}_k(t_k^+)) \exp[\eta_k(t - t_k)]. \quad (16)$$

From inequality (15), when $t \in (t_k + \theta T, t_k + \theta T + T/2)$, let $t = t_k + \theta T + T/2$. So,

$$\begin{aligned} V_k(\mathbf{e}_k(t)) &\leq \lambda_k^\theta V_k(\mathbf{e}_k(t_k^+)) \exp[\eta_k(\theta T + T/2)] \\ &\leq \exp(\theta \ln \lambda_k) V_k(\mathbf{e}_k(t_k^+)) \exp[\eta_k(\theta T + T/2)] \\ &\leq V_k(\mathbf{e}_k(t_k^+)) \exp[\theta \ln \lambda_k + \theta \eta_k T + \eta_k T/2] \\ &\leq V_k(\mathbf{e}_k(t_k^+)) \exp[\theta(\ln \lambda_k + \eta_k T) + \eta_k T/2]. \end{aligned} \quad (17)$$

From inequality (16), when $t \in [t_k + \theta T + T/2, t_k + (\theta + 1)T]$, let $t = t_k + (\theta + 1)T$. So,

$$\begin{aligned} V_k(\mathbf{e}_k(t)) &\leq \lambda_k^{\theta+1} V_k(\mathbf{e}_k(t_k^+)) \exp[\eta_k((\theta + 1)T)] \\ &\leq \exp[(\theta + 1) \ln \lambda_k] V_k(\mathbf{e}_k(t_k^+)) \\ &\quad \cdot \exp[\eta_k((\theta + 1)T)] \\ &\leq V_k(\mathbf{e}_k(t_k^+)) \exp[(\theta + 1) \ln \lambda_k \\ &\quad + \eta_k((\theta + 1)T)] \\ &\leq V_k(\mathbf{e}_k(t_k^+)) \exp[(\theta + 1)(\ln \lambda_k + \eta_k T)]. \end{aligned} \quad (18)$$

We know that the k^{th} agent group starts working at time t_k , so $\mathbf{e}_k(t_k^+)$ is the initial value of the error system $\mathbf{e}_k(t)$. From inequalities (17) and (18) and the conditions of Theorem 1, we conclude that when $t \rightarrow +\infty$, we have $\theta + 1 \rightarrow +\infty$. So, $\lim_{t \rightarrow +\infty} V_k(\mathbf{e}_k(t)) = 0$.

6 Example

Considering the central idea of this study, we give a numerical example to verify the availability and reliability of the proposed model. We consider that there is one leader agent and four agent groups. The leader agent is x_0 , the first agent group is x_1 , the second agent group is x_2 , the third agent group is x_3 , and the fourth agent group is x_4 . At $t_0 = 0$, assume that the leader agent starts working. The k^{th} ($k = 1, 2, 3, 4$) agent group is dynamically joined at time t_k ($0 < t_1 \leq t_2 \leq t_3 \leq t_4 < +\infty$).

Fig. 7 shows the working time of the leader agent x_0 and the dynamic join time of the four agent groups x_1, x_2, x_3 , and x_4 .

Let $H = 3.2$ and $\varphi(x_0(t)) = \sqrt{x_0^2(t) + 5}$. The dynamics of the leader agent x_0 is as follows:

$$\dot{x}_0(t) = 3.2x_0(t) + \sqrt{x_0^2(t) + 5}, \quad (19)$$

and let $x_0(t_0) = x_0(0) = 0.237$ to represent the initial state of the leader agent.

From Fig. 7, we can see that the first agent group has two agents, x_{11} and x_{12} . The second agent group has two agents, x_{21} and x_{22} . The third agent group has three agents, x_{31} , x_{32} , and x_{33} . The fourth agent group has one agent x_{41} . The directed edge ε_1 roots at x_0 and ends at x_{11} . The directed edge ε_2 roots at x_0 and ends at x_{21} . The directed edges $\varepsilon_3, \varepsilon_4$, and ε_5 all root at x_0 and end at x_{31}, x_{32} , and x_{33} , respectively. The directed edge ε_6 roots at x_0 and ends at x_{41} .

From Fig. 7, we can obtain

$$L_1 = \begin{bmatrix} 1 & -1 \\ -1 & 1 \end{bmatrix}, L_2 = \begin{bmatrix} 1 & -1 \\ -1 & 1 \end{bmatrix},$$

$$L_3 = \begin{bmatrix} 2 & -1 & -1 \\ -1 & 2 & -1 \\ -1 & -1 & 2 \end{bmatrix}, L_4 = [0],$$

$$B_1 = \begin{bmatrix} 1 & 0 \\ 0 & 0 \end{bmatrix}, B_2 = \begin{bmatrix} 1 & 0 \\ 0 & 0 \end{bmatrix},$$

$$B_3 = \begin{bmatrix} 1 & 0 & 0 \\ 0 & 1 & 0 \\ 0 & 0 & 1 \end{bmatrix}, B_4 = [1].$$

Similarly, $\varphi(x_{ki}(t)) = \sqrt{x_{ki}^2(t) + 5}$ and the dynamics of the i^{th} agent in the k^{th} agent group is

$$\begin{aligned} \dot{x}_{ki}(t) = & 3.2x_{ki}(t) + \sqrt{x_{ki}^2(t) + 5} \\ & + \sum_{m=1}^{\infty} f_k \left(\sum_{kj \in \Xi_{ki}} a_{kij} [x_{ki}(t) - x_{kj}(t)] \right. \\ & \left. + b_{ki} [x_{ki}(t) - x_0(t)] \right) \delta(t - t_{km}), \\ & k = 1, 2, 3, 4, m = 0, 1, \dots \end{aligned} \quad (20)$$

When $k = 1$ then $i = 1, 2$, when $k = 2$ then $i = 1, 2$, when $k = 3$ then $i = 1, 2, 3$, and when $k = 4$ then $i = 1$. From Theorem 1 and the central idea of this study, let $f_1 = -0.18, f_2 = -0.198, f_3 = -0.33$, and $f_4 = -1.28$. We use Matlab to simulate all agent groups. Let the system control period $T = 0.03$ s and the step size $p = 0.0015$ s. Let $t_1 = 20p = 0.03$ s, $t_2 = 50p = 0.075$ s, $t_3 = 70p = 0.105$ s, $t_4 = 90p = 0.135$ s. The initial values of all agent groups are

$$\begin{aligned} x_{11}(0.03) &= 1.2, x_{12}(0.03) = -1.2, \\ x_{21}(0.075) &= 1.1, x_{22}(0.075) = 0.2, \\ x_{31}(0.105) &= 1.65, x_{32}(0.105) = 1.3, \\ x_{33}(0.105) &= -0.52, x_{41}(0.135) = -1.58. \end{aligned}$$

This example assumes that the state value of each agent group from time 0 to its initial time is always equal to its initial state value. Through the above initial values and parameter setting, we can obtain four exponentially stable solutions. Figs. 8–11 show the state error values between the leader agent and the first, second, third, and fourth agent groups, respectively, all expressed over time.

Figs. 12–15 show the state values of the first, second, third, and fourth agent groups. It can be seen from Figs. 8–15 that system (20) has achieved state consensus; that is, all agent groups have achieved state consensus with dynamic join characteristics under impulsive control.

7 Conclusions

We have studied the state consensus problem of multi-agent systems with dynamic join

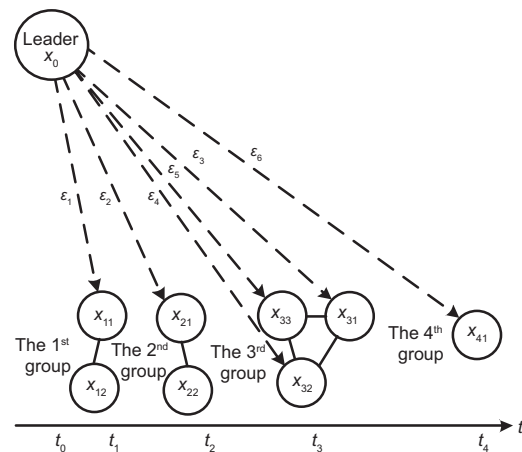


Fig. 7 Working time of the leader agent x_0 and the dynamic join time of the four agent groups x_1, x_2, x_3 , and x_4

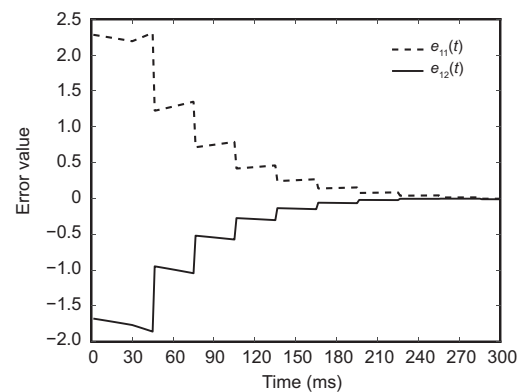


Fig. 8 State error between the first agent group and the leader agent

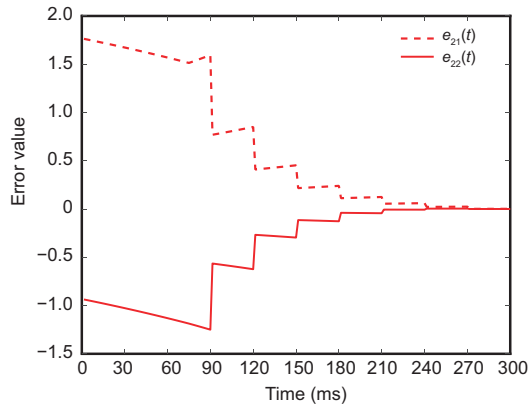


Fig. 9 State error between the second agent group and the leader agent

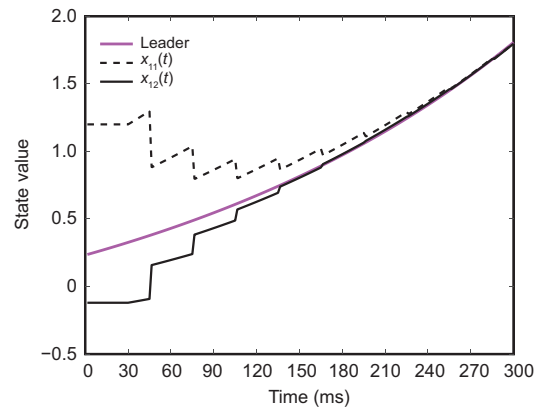


Fig. 12 State value of the first group

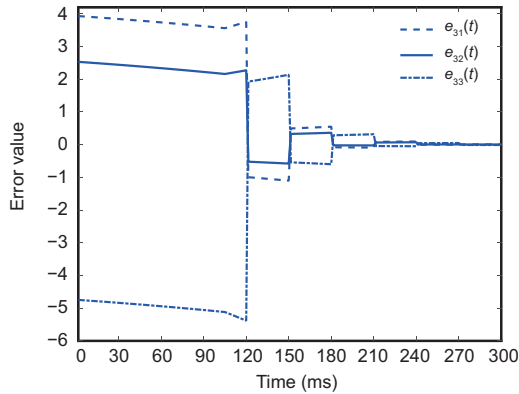


Fig. 10 State error between the third agent group and the leader agent

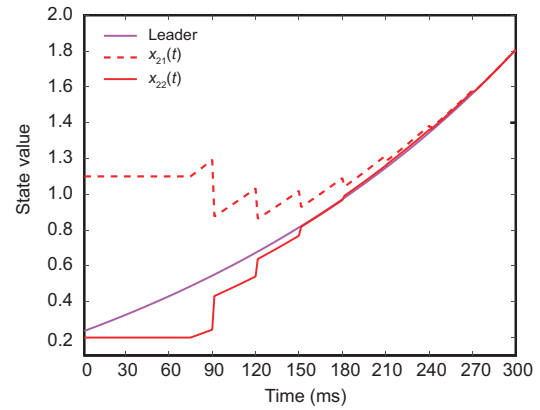


Fig. 13 State value of the second group

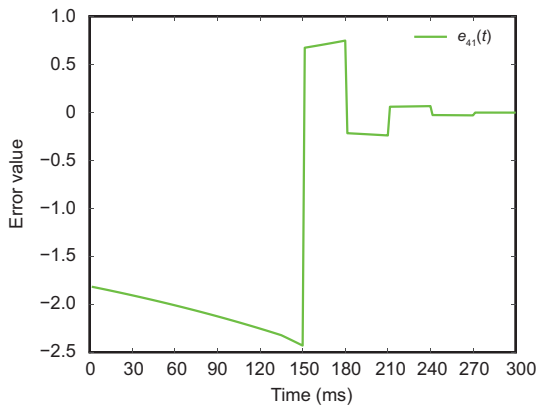


Fig. 11 State error between the fourth agent group and the leader agent

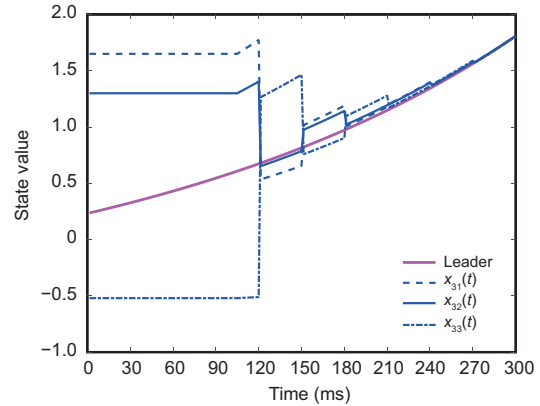


Fig. 14 State value of the third group

characteristics under impulsive control. To the best of our knowledge, we have given the definition of dynamic join characteristics of multi-agent systems for the first time. We have divided the schemes of the state consensus of multi-agent systems with dynamic join characteristics into four cases. We have obtained four feasible schemes in theory, including the best one for actual industrial production.

Compared with other feasible schemes, this scheme has more advantages in communication, and has the advantage of unified form for the state consensus problem of single group and multiple groups in control; thus, it has higher practicability. Based on the best scheme, we have established the dynamic models of agent groups. In addition, the error system $e_k(t)$ between the agent groups and the leader agent has been obtained. We have used the Lyapunov

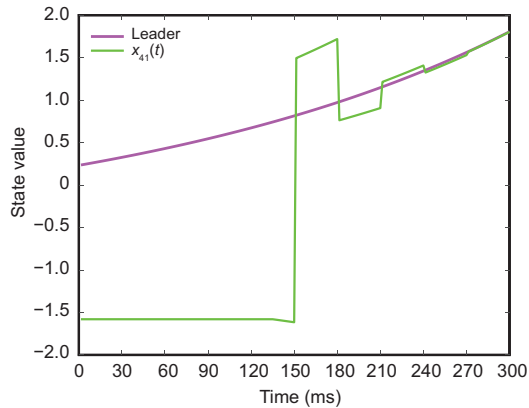


Fig. 15 State value of the fourth group

stability theory to analyze the error system $e_k(t)$, and obtained the necessary and sufficient conditions for the exponential stability of the error system $e_k(t)$, that is, Theorem 1. Finally, a numerical example has been given to verify the practicality and validity of Theorem 1. The idea and theorem are of significance in industrial production and can be widely used in industry.

Contributors

Xiang HU designed the research. Xiang HU and Zufan ZHANG processed the data. Xiang HU drafted the manuscript. Chuandong LI helped organize the manuscript and provided important guidance in the theoretical derivation and experimental design. Xiang HU and Chuandong LI revised and finalized the paper.

Compliance with ethics guidelines

Xiang HU, Zufan ZHANG, and Chuandong LI declare that they have no conflict of interest.

References

- Cao YF, Sun YG, 2016. Consensus of third-order multiagent systems with time delay in undirected networks. *Math Probl Eng*, 2016:6803927. <https://doi.org/10.1155/2016/6803927>
- Cheng S, Dong H, Yu L, et al., 2019. Consensus of second-order multi-agent systems with directed networks using relative position measurements only. *Int J Contr Autom Syst*, 17(1):85-93. <https://doi.org/10.1007/s12555-018-0148-0>
- Geng HL, Duan GR, 2007. Stability of linear constant system with linear impulse. *Chinese Control Conf*, p.76-79. <https://doi.org/10.1109/CHICC.2006.4347405>
- Han YY, Li CD, 2018. Second-order consensus of discrete-time multi-agent systems in directed networks with nonlinear dynamics via impulsive protocols. *Neurocomputing*, 286:51-57. <https://doi.org/10.1016/j.neucom.2018.01.053>

- Hao F, Chen X, 2012. Event-triggered average consensus control for discrete-time multi-agent systems. *IET Contr Theory Appl*, 6(16):2493-2498. <https://doi.org/10.1049/iet-cta.2011.0535>
- Hu W, Zhu QX, 2018. Moment exponential stability of stochastic nonlinear delay systems with impulse effects at random times. *Int J Rob Nonl Contr*, 29(12):3809-3820. <https://doi.org/10.1002/rnc.4031>
- Huang C, Zhang X, Lam H, et al., 2020. Synchronization analysis for nonlinear complex networks with reaction-diffusion terms using fuzzy-model-based approach. *IEEE Trans Fuzzy Syst*, in press. <https://doi.org/10.1109/TFUZZ.2020.2974143>
- Huang J, Cao M, Zhou N, et al., 2017. Distributed behavioral control for second-order nonlinear multi-agent systems. *IFAC-PapersOnLine*, 50(1):2445-2450. <https://doi.org/10.1016/j.ifacol.2017.08.407>
- Huang TW, Li CD, Duan SK, et al., 2012. Robust exponential stability of uncertain delayed neural networks with stochastic perturbation and impulse effects. *IEEE Trans Neur Netw Learn Syst*, 23(6):866-875. <https://doi.org/10.1109/TNNLS.2012.2192135>
- Jiang FC, Wang L, Xie GM, 2010. Consensus of high-order dynamic multi-agent systems with switching topology and time-varying delays. *J Contr Theory Appl*, 8(1):52-60. <https://doi.org/10.1007/s11768-010-9184-x>
- Lee K, Bhattacharya R, 2016. Convergence analysis of asynchronous consensus in discrete-time multi-agent systems with fixed topology. <https://arxiv.org/abs/1606.04156>.
- Li CJ, Liu GP, 2018a. Consensus for heterogeneous networked multi-agent systems with switching topology and time-varying delays. *J Franklin Inst*, 355(10):4198-4217. <https://doi.org/10.1016/j.jfranklin.2018.04.003>
- Li CJ, Liu GP, 2018b. Data-driven leader-follower output synchronization for networked non-linear multi-agent systems with switching topology and time-varying delays. *J Syst Sci Compl*, 31(1):87-102. <https://doi.org/10.1007/s11424-018-7269-7>
- Li XD, Zhang XL, Song SJ, 2017. Effect of delayed impulses on input-to-state stability of nonlinear systems. *Automatica*, 76:378-382. <https://doi.org/10.1016/j.automatica.2016.08.009>
- Li YL, Li HT, Ding XY, et al., 2019. Leader-follower consensus of multiagent systems with time delays over finite fields. *IEEE Trans Cybern*, 49(8):3203-3208. <https://doi.org/10.1109/TCYB.2018.2839892>
- Li YM, Sun YY, Hua J, et al., 2015. Indirect adaptive type-2 fuzzy impulsive control of nonlinear systems. *IEEE Trans Fuzzy Syst*, 23(4):1084-1099. <https://doi.org/10.1109/TFUZZ.2014.2346235>
- Liu XL, Xiao JW, Chen DX, et al., 2019. Dynamic consensus of nonlinear time-delay multi-agent systems with input saturation: an impulsive control algorithm. *Nonl Dynam*, 97(2):1699-1710. <https://doi.org/10.1007/s11071-019-05098-z>
- Lu ZH, Zhang L, Wang L, 2019. Controllability analysis of multi-agent systems with switching topology over finite fields. *Sci China Inform Sci*, 62(1):12201. <https://doi.org/10.1007/s11432-017-9284-4>
- Luo J, Cao CY, 2015. Flocking for multi-agent systems with unknown nonlinear time-varying uncertainties under a

- fixed undirected graph. *Int J Contr*, 88(5):1051-1062. <https://doi.org/10.1080/00207179.2014.992963>
- Schoukens J, Godfrey K, Schoukens M, 2018. Nonparametric data-driven modeling of linear systems: estimating the frequency response and impulse response function. *IEEE Contr Syst Mag*, 38(4):49-88. <https://doi.org/10.1109/MCS.2018.2830080>
- Sesekin AN, Nepp AN, 2015. Impulse position control algorithms for nonlinear systems. 41st Int Conf on Applications of Mathematics in Engineering and Economics, p.040002-1-040002-5. <https://doi.org/10.1063/1.4936709>
- Shahrrava B, 2018. Closed-form impulse responses of linear time-invariant systems: a unifying approach [lecture notes]. *IEEE Signal Process Mag*, 35(4):126-132. <https://doi.org/10.1109/MSP.2018.2810300>
- Shang YL, 2012. Finite-time consensus for multi-agent systems with fixed topologies. *Int J Syst Sci*, 43(3):499-506. <https://doi.org/10.1080/00207721.2010.517857>
- Shi M, Yu YJ, Xu Q, 2019. Delay-dependent consensus condition for a class of fractional-order linear multi-agent systems with input time-delay. *Int J Syst Sci*, 50(4):669-678. <https://doi.org/10.1080/00207721.2019.1567865>
- Wang AJ, Liao XF, He HB, 2019. Event-triggered differentially private average consensus for multi-agent network. *IEEE/CAA J Autom Sin*, 6(1):75-83. <https://doi.org/10.1109/JAS.2019.1911327>
- Wang H, Yu WW, Wen GH, et al., 2018. Finite-time bipartite consensus for multi-agent systems on directed signed networks. *IEEE Trans Circ Syst I*, 65(12):4336-4348. <https://doi.org/10.1109/TCSI.2018.2838087>
- Wang H, Yu WW, Ren W, et al., 2019. Distributed adaptive finite-time consensus for second-order multiagent systems with mismatched disturbances under directed networks. *IEEE Trans Cybern*, in press. <https://doi.org/10.1109/TCYB.2019.2903218>
- Wang JR, Luo ZJ, Shen D, 2018. Iterative learning control for linear delay systems with deterministic and random impulses. *J Franklin Inst*, 355(5):2473-2497. <https://doi.org/10.1016/j.jfranklin.2018.01.013>
- Wang S, Xie D, 2012. Consensus of second-order multi-agent systems via sampled control: undirected fixed topology case. *IET Contr Theory Appl*, 6(7):893-899. <https://doi.org/10.1049/iet-cta.2011.0282>
- Wang X, Li CD, Huang TW, et al., 2014. Impulsive control and synchronization of nonlinear system with impulse time window. *Nonl Dynam*, 78(4):2837-2845. <https://doi.org/10.1007/s11071-014-1629-1>
- Wang XM, Wang T, Xu CB, et al., 2018. Average consensus for multi-agent system with measurement noise and binary-valued communication. *Asian J Contr*, 21(3):1043-1056. <https://doi.org/10.1002/asjc.1801>
- Wang YQ, Lu JQ, Lou YJ, 2019. Halanay-type inequality with delayed impulses and its applications. *Sci China Inf Sci*, 62(9):192206. <https://doi.org/10.1007/s11432-018-9809-y>
- Wang ZM, Zhang H, Wang WS, 2016. Robust consensus for linear multi-agent systems with noises. *IET Contr Theory Appl*, 10(17):2348-2356. <https://doi.org/10.1049/iet-cta.2016.0191>
- Wen GG, Zhang YL, Peng ZX, et al., 2019. Observer-based output consensus of leader-following fractional-order heterogeneous nonlinear multi-agent systems. *Int J Contr*, in press. <https://doi.org/10.1080/00207179.2019.1566636>
- Wen GH, Zheng WX, 2019. On constructing multiple Lypunov functions for tracking control of multiple agents with switching topologies. *IEEE Trans Autom Contr*, 64(9):3796-3803. <https://doi.org/10.1109/TAC.2018.2885079>
- Wu T, Hu J, Chen DY, 2019. Non-fragile consensus control for nonlinear multi-agent systems with uniform quantizations and deception attacks via output feedback approach. *Nonl Dynam*, 96(1):243-255. <https://doi.org/10.1007/s11071-019-04787-z>
- Xie DM, Wang SK, 2012. Consensus of second-order discrete-time multi-agent systems with fixed topology. *J Math Anal Appl*, 387(1):8-16. <https://doi.org/10.1016/j.jmaa.2011.08.052>
- Xu Y, Luo DL, Li DY, et al., 2019. Affine formation control for heterogeneous multi-agent systems with directed interaction networks. *Neurocomputing*, 330(22):104-115.
- Ye YY, Su HS, 2019. Leader-following consensus of nonlinear fractional-order multi-agent systems over directed networks. *Nonl Dynam*, 96(2):1391-1403. <https://doi.org/10.1007/s11071-019-04861-6>
- Yuan S, Cheng Z, Lei G, 2018. Uncoupled PID control of coupled multi-agent nonlinear uncertain systems. *J Syst Sci Compl*, 31(1):4-21. <https://doi.org/10.1007/s11424-018-7335-1>
- Zhai SD, Yang XS, 2014. Consensus of second-order multi-agent systems with nonlinear dynamics and switching topology. *Nonl Dynam*, 77(4):1667-1675. <https://doi.org/10.1007/s11071-014-1408-z>
- Zhang WB, Ho DWC, Tang Y, et al., 2019. Quasi-consensus of heterogeneous-switched nonlinear multi-agent systems. *IEEE Trans Cybern*, in press. <https://doi.org/10.1109/TCYB.2018.2882191>
- Zhang Y, Tian YP, 2014. Allowable delay bound for consensus of linear multi-agent systems with communication delay. *Int J Syst Sci*, 45(10):2172-2181. <https://doi.org/10.1080/00207721.2013.763303>
- Zheng M, Liu CL, Liu F, 2019. Average-consensus tracking of sensor network via distributed coordination control of heterogeneous multi-agent systems. *IEEE Contr Syst Lett*, 3(1):132-137. <https://doi.org/10.1109/LCSYS.2018.2856105>
- Zhou B, Liao XF, 2014. Leader-following second-order consensus in multi-agent systems with sampled data via pinning control. *Nonl Dynam*, 78(1):555-569. <https://doi.org/10.1007/s11071-014-1460-8>
- Zhu W, Wang DD, Zhou QH, 2019. Leader-following consensus of multi-agent systems via adaptive event-based control. *J Syst Sci Compl*, 32(3):846-856. <https://doi.org/10.1007/s11424-018-7177-x>
- Zou WC, Xiang ZR, Ahn CK, 2019. Mean square leader-following consensus of second-order nonlinear multi-agent systems with noises and unmodeled dynamics. *IEEE Trans Syst Man Cybern Syst*, 49(12):2478-2486. <https://doi.org/10.1109/TSMC.2018.2862140>